Voltage shifts and defect-dipoles in ferroelectric capacitors

W. L. Warren, G. E. Pike, D. Dimos, K. Vanheusden, H.N. Al-Shareef, B. A. Tuttle, R. Ramesh* and J. T. Evans, Jr.**

Sandia National Laboratories, Albuquerque, New Mexico 87185-1349
** Department of Materials and Nuclear Engineering, University of Maryland, College Park, Maryland 20742*
*** Radiant Technologies Inc., 1009 Bradbury Ave., Albuquerque, New Mexico 87106*

ABSTRACT

We review the processes and mechanisms by which voltage offsets occur in the hysteresis loop of ferroelectric materials. Simply stated, voltage shifts arise from near-interfacial charge trapping in the ferroelectric. We show that the impetus behind voltage shifts in ferroelectric capacitors is the *net* polarization, with the net polarization being determined by the perovskite and the aligned defect-dipole components. Some common defect-dipoles in the PZT system are lead vacancy-oxygen vacancy complexes. One way to change the net polarization in the ferroelectric is to subject the PZT capacitor to a dc bias at elevated temperature; this process is spectroscopically shown to align defect-dipoles along the direction of the applied electric field. The alignment of defect-dipoles can strongly impact several material properties. One such impact is that it can lead to enhanced voltage shifts (imprint). It is proposed that the net polarization determines the spatial location of the asymmetrically trapped charge that are the cause for the voltage shifts. An enhanced polarization at one electrode interface can lead to larger voltage shifts since it lowers the electrostatic potential well for electron trapping, i.e., more electron trapping can occur. Defect-dipole alignment is also shown to increase the UV sensitivity of the ferroelectric.

INTRODUCTION

Even though many technologically important device properties stem from the polarization exhibited in ferroelectric materials [1-3], it is somewhat incongruous that the polarization itself can be linked to various forms of degradation of device performance [4-7]. For instance, when a ferroelectric capacitor is left in a particular polarization state for a period of time, voltage shifts can occur in the hysteresis loop as illustrated in Fig. 1 [4-6,8-17]. The development of a voltage shift in thin films left in a given polarization state is the basis of the phenomenon of imprint [6], which is used to describe the failure of capacitors in nonvolatile memories. A voltage shift can lead to 'read' failure of a memory element if the shift is large enough that the difference in the value of the polarization between the two remanent states drops below a threshold value. For example, the difference between $+P_r$ and $-P_r$ for the shifted loop in Fig. 1 is much smaller than for the initial case. A 'write' failure mechanism also can occur if the voltage shift increases the coercive voltage in one direction such that the ferroelectric cannot be switched by the programming voltage. Besides, thermal treatments, voltage shifts can also occur by illuminating a poled or biased capacitor with bandgap light [4].

These voltage shifts are key reliability issues for ferroelectric non-volatile memories [6,18], and bulk ferroelectric capacitors [9-16]. In this paper, we discuss imprint with particular emphasis on the interaction between domains and charge trapping and the role of the doubly positively charged oxygen vacancies ($V_O^{\bullet\bullet}$) and its associated defect-dipoles.

DISCLAIMER

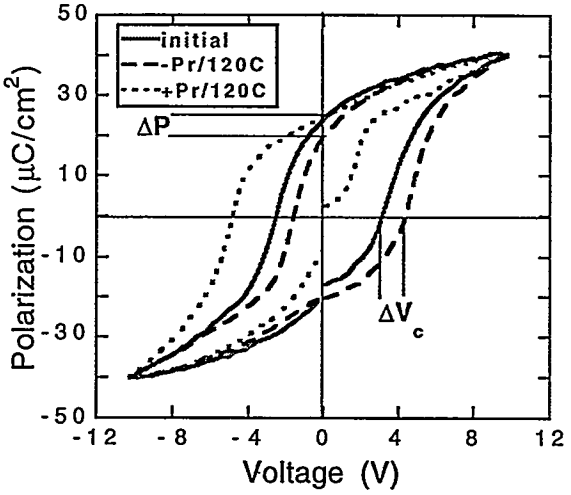

Figure 1: Hysteresis loops for a PZT 30/70 film illustrating a thermally-induced voltage shift obtained by heating at $\pm P_r$ and 120°C for 2 hrs.

EXPERIMENTAL DETAILS

The Si wafer substrates were prepared with either rf sputter deposited Pt, RuO_2, or $La_{0.5}Sr_{0.5}CoO_3$ (LSCO) electrodes. The $Pb(Zr_x,Ti_{1-x})O_3$ thin films (x = 0.3 or 0.45) were prepared using a sol-gel approach [19]. The PZT sol-gel solutions were spin deposited onto the substrates and then pyrolyzed for 5 min. at 300°C. Sequential spin depositions and dry steps were followed by an anneal for 30 min. at 675°C in air to crystallize the PZT film. The top electrode consisted of a sputter deposited array of 50 or 100 μm Pt, RuO_2 or LSCO dots. The polarization-voltage (P-V) measurements were made at room temperature with a Radiant Technologies RT-66A tester. An Oriel Hg arc lamp was used to optically illuminate the samples with ultra-violet (UV) light at 300 K.

The $BaTiO_3$ ceramics (typically all 6 mm long, 1 mm thick and 2 mm wide) were all prepared by hot pressing techniques. Indium tin oxide electrodes were sputter deposited on the samples for electrical contact and then annealed at 500°C to increase their conductivity. Dielectric measurements on the capacitors were made using a Hewlett Packard LCR meter. The capacitance was measured at 10 kHz. Polarization-voltage (P-V) loops for the ceramics were measured using the RT-66A tester in conjunction with a high voltage interface.

The EPR measurements on the $BaTiO_3$ ceramics were made with an *X*-band Bruker ESP-300E spectrometer at 20K. At 300 K (20 K) the $BaTiO_3$ ceramic exhibits tetragonal (rhombohedral) symmetry. A small ($10^{18}/cm^3$) concentration of isolated Fe^{3+} centers were observed in the $BaTiO_3$ ceramics. The samples were not deliberately doped with Fe impurities.

RESULTS AND DISCUSSION

The driving force for voltage shifts

Dimos and co-workers have shown that voltage shifts in thin films arise from an asymmetric distribution of trapped charge [4], more specifically trapped electrons. Strong

support for the involvement of the polarization in the creation of a voltage shift is that the sign of the voltage shift depends on the sign of the polarization state [4-6], i.e., poling the capacitor to $-P_r$ ($+P_r$) and either heating it, or illuminating it with bandgap light, will induce a positive (negative) voltage shift in the hysteresis loop (Fig. 1). Furthermore, it has been shown that for films with nearly square hysteresis loops that the photo-induced voltage shift was essentially the same at remanence and at saturating bias which also argues that the polarization state is the driving force for the charge trapping [4], i.e., the voltage shifts. Somewhat analogously, we further advance the involvement of the polarization in imprint and aging by varying the remanent polarization in a controlled and systematic manner to determine its impact on the thermally-induced voltage shifts. To vary P_r, films were initialized by heating above the Curie temperature, then minor hysteresis loops were taken at room temperature with differing maximum biases to set P_r. Next, voltage shifts were induced by keeping the capacitor in a particular remanence polarization state and subsequently heating it to 120°C for 2 hrs. By measuring the average of the coercive voltages at room temperature, the voltage offset, or the internal bias voltage (V_i) was determined. Figure 2 shows that the value of the remanent polarization strongly effects V_i; the larger the polarization, the greater the voltage shift. This observation demonstrates a direct link between the magnitude of the remanent polarization of the ferroelectric and the voltage shift.

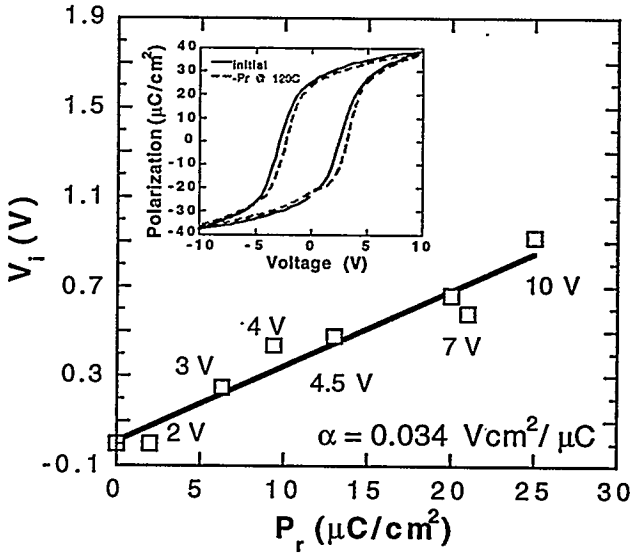

Figure 2: Thermally-induced internal bias voltage for various values of P_r. P_r was varied by poling the capacitor to different amounts. The voltage shifts were induced by keeping the capacitor in a particular $-P_r$ state and then heating it to 120°C for 2 hrs. Inset: Hysteresis loops for a PZT 40/60 film illustrating a thermally-induced voltage shift obtained by heating at $-P_r$ and 120°C for 2 hrs.

The connection between P_r and V_i is in good agreement with the voltage offset model proposed by Dimos et al. [4]. This model proposed that near-interfacial trapped electrons (which lead to the voltage shifts) are attracted by the electrostatic potential well at the positive head of the polarization. Pike et al. [5] showed that the density of trapped electrons is dependent on the *net* polarization, where the net polarization is comprised of two components - the "normal" ferroelectric polarization, P_r, and a volumetric distribution of aligned defect-dipole complexes in the material [9,11,12,16,20,21] denoted as P_D. An

enhanced net polarization can lead to greater charge trapping since it will lower the electrostatic potential well for charge capture. Aligned defect-dipole complexes include defects such as $V_O^{\bullet\bullet}$ associated with lead vacancies (V''_{Pb} - $V_O^{\bullet\bullet}$) [22,23] or Fe centers. The Fe centers are defect-dipoles in that the Fe ions have substituted for the Ti^{4+} ion and are negatively charged and the $V_O^{\bullet\bullet}$ is doubly positively charged with respect to the neutral lattice [23-27]. The lead vacancy is doubly negatively charged with respect to the neutral lattice. The V''_{Pb} $-V_O^{\bullet\bullet}$ complex is likely in PZT dielectrics due to the inherent PbO loss during high-temperature treatments.

Defect-dipole alignment

Thus, the voltage shift model of Pike et al. [5] incorporating defect-dipoles is based on the premise that defect-dipole alignment can occur in ferroelectric materials, and that it can contribute significantly to the net polarization state. In light of this, we now discuss the characteristics of defect-dipole alignment.

The concept of defect-dipole alignment was first suggested by Lambeck and Jonker [9,16] in which they proposed that the defect-dipoles can become aligned along the direction of the spontaneous polarization. They further proposed that dielectric aging is due to a gradual alignment of doubly positively charged oxygen-vacancy ($V_O^{\bullet\bullet}$) associated defect-dipoles in the perovskite lattice. Arlt and co-workers [11,12,21] have provided a quantitative model describing the kinetics of defect-dipole alignment and have also proposed that defect-dipole alignment is intimately involved in ferroelectric aging.

However, the evidence for defect-dipole alignment was only recently demonstrated. Using electron paramagnetic resonance, we have been able to unambiguously demonstrate that *prolonged* bias stress conditions aligns defect-dipoles along the applied external field direction in both $BaTiO_3$ and PZT materials [21,28]. The alignment was shown to occur via orientational dependent EPR centers in a *polycrystalline* lattice. As one example, these measurements have shown that the alignment of Fe^{3+}-$V_O^{\bullet\bullet}$ dipoles in $BaTiO_3$ ceramics is essentially complete after less than 2 hours at 110°C and 4.5 kV/cm. A schematic of unaligned and aligned defect-dipoles, specifically V_{Pb}''-$V_O^{\bullet\bullet}$ dipoles are illustrated in Fig. 3.

Electrically speaking, the alignment of the defect-dipoles should enhance the polarization along the applied electric field direction, and thus cause a polarization offset in the hysteresis loop. However, normal polarization-voltage (P-V) hysteresis loops are not able to distinguish this enhanced polarization since they only sense the polarization that can be switched during the time scale of the measurement. Hysteresis loops do not measure the magnitude of the polarization in either the initial or final state. The defect-dipole component to the polarization can not respond to the time scale of the room temperature P-V measurements, hence, the P-V loops are only a measure of the switchable perovskite polarization. The situation is further exacerbated since the position of the P-V loop on the polarization axis is historically (and artificially) situated symmetric about 0 $\mu C/cm^2$.

To overcome this ambiguity strain-voltage (S-V) measurements were taken before and after bias/thermal combinations [29]. Complementary S-V measurements provide information regarding the position of the P-V loop along the polarization axis. Qualitatively, if the strain measurements show the typical symmetric "butterfly" loops, then the P-V loop is placed symmetrically about 0 $\mu C/cm^2$. However, if the strain measurements are asymmetric, being greater at negative voltages, then the P-V loop will

be displaced with negative polarization values. This displaced P-V loop indicates that there is a additional polarization that is not switched by the room-temperature P-V measurement, but is sensed by the additional displacement detected in the S-V measurements. These results [29] have shown that aligned defect-dipoles also lead to an enhanced polarization state through bias/thermal combinations. The prolonged bias/temperature stress is necessary to re-orientate and thus, switch the defect-dipoles [20,30]. The result being that alignment causes the hysteresis loop to be offset along the polarization axis as schematically shown in Fig. 3. Thus, we conclude that defect-dipole alignment can occur in ferroelectric materials and it does lead to a polarization offset.

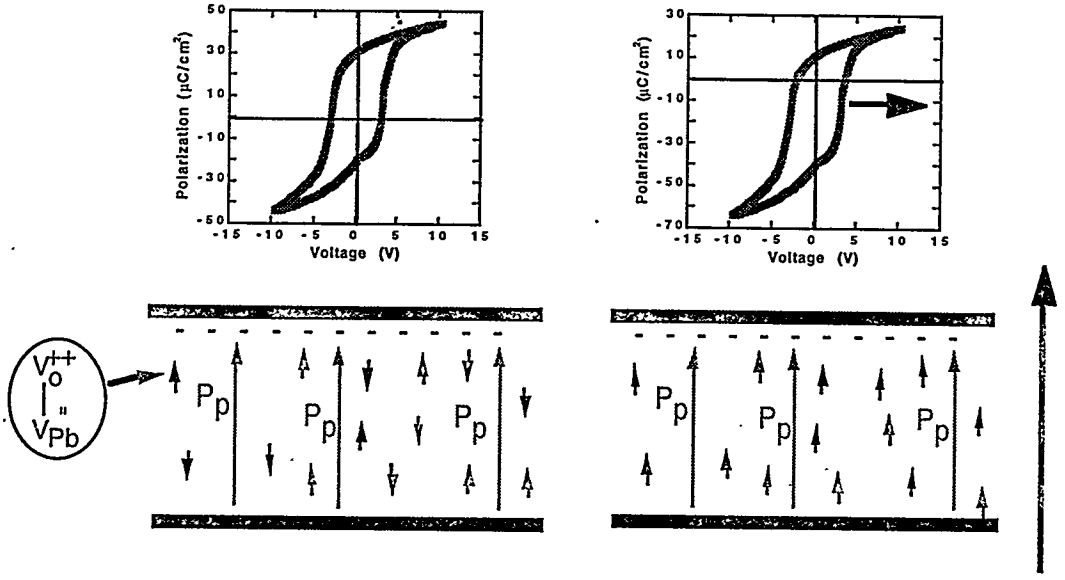

Figure 3: (A) Schematic P-V loop and randomized defect-dipoles of a PZT thin film that has been poled to $-P_r$ at room temperature. (B) Schematic P-V loop and aligned defect-dipoles of a PZT thin film following a negative saturating bias/120°C combination. The bias combination leads to polarization offset, and the potential for an enhanced voltage offset due to the alignment of defect-dipoles.

Defect-dipoles and voltage shifts

Several investigators have proposed that voltage shifts are due to defect-dipoles; more specifically, voltage offsets are considered to be a bulk effect and are caused only by the orientation (alignment) of defect-dipoles [9,11,12,16,21]. There are a number of compelling reasons why this model is questionable. One theoretical and two experimental refutations are given below.

(1) To the extent that electron trapping is linearly proportional to the net polarizations (Fig. 2), the unswitched defect-dipole polarization will fix the trapped charge and this charge will not be manifest in the P-V loop.

(2) Voltage shifts measured by offsets in the hysteresis loop can occur without preferentially aligned defect-dipoles as measured via EPR (Fig. 4). The voltage shift was induced by heating a $BaTiO_3$ capacitor at 65°C under remanence (no applied bias) and the defect-dipole that was monitored via EPR was the Fe^{3+}-$V_O^{\bullet\bullet}$ complex. It has been suggested that $V_O^{\bullet\bullet}$-related defect-dipoles align by $V_O^{\bullet\bullet}$ motion in the octahedron about the complex, with the motion being driven by the applied field with thermal assistance [30]. As shown in Fig. 5, defect-dipole alignment is only manifested under the presence of an applied electric field; it does *not* occur under remanence. The alignment kinetics are found to be both temperature

and field dependent. The temperature dependence is described by a normalized exponential function:

Fraction of [Fe^{3+}-$V_O^{\bullet\bullet}$] aligned normal to the electrodes = [1 - 2/3exp(-t/τ)]

Earlier [30] from an Arrhenius plot (ln τ vs. 1/T) the $V_O^{\bullet\bullet}$ motion was found to be characterized by an activation energy of 0.91 eV, close to that predicted for $V_O^{\bullet\bullet}$ motion in the perovskite lattice [31-33].

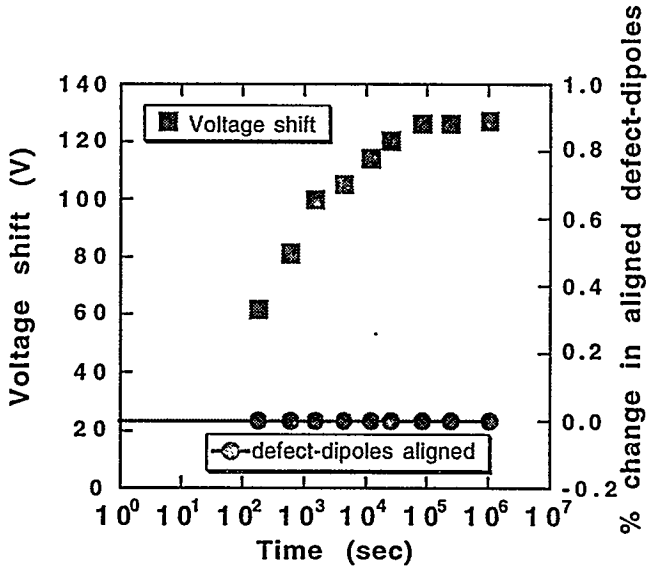

Figure 4: Internal bias field and percentage change in aligned defect-dipoles following a $-P_r$/65°C combination for various times in a $BaTiO_3$ ceramic capacitor. The internal bias field was measured by the voltage offset in the hysteresis loop and the aligned defect-dipoles were determined by EPR.

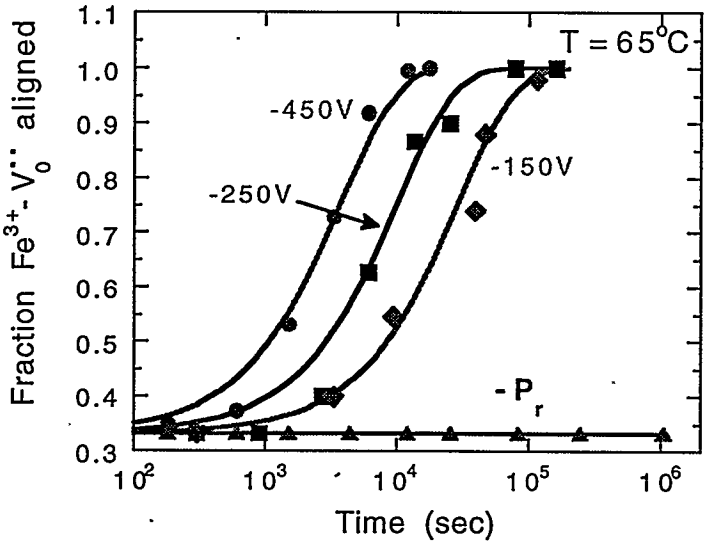

Figure 5: Alignment kinetics for the Fe^{3+}-$V_O^{\bullet\bullet}$ complex at different applied voltages. The temperature during the bias was 65°C. The data are fit to the expression in eqn. (1).

Figure 6 shows the relationship between τ and the applied voltage:

$$\tau \alpha V^{-1.9}.$$

The relationships among τ and V and T found here are essentially identical to those modeled for resistance degradation by Waser [32,34] and the lifetime of high dielectric constant multilayer capacitors by Minford [35], indicating that all three phenomena are a consequence of $V_o^{\bullet\bullet}$ motion in the lattice.

(3) Dimos and Warren [29] have shown using strain-voltage measurements that voltage shifts are not necessarily observed in PZT ceramics, even though significant defect-dipole alignment has occurred. For example, they found that no voltage shift was induced by subjecting a PZT bulk capacitor to -1000V/120°C combination even though this process generated a polarization offset of 40 $\mu C/cm^2$! Collectively these two extremes rule out the notion that aligned defect-dipoles in and of themselves are the cause of voltage offsets.

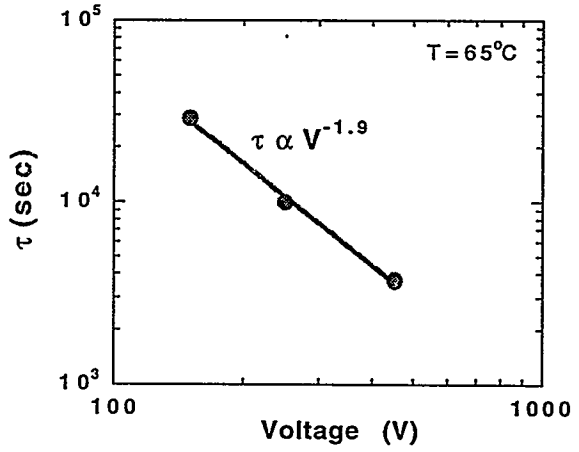

Figure 6: Log-log plot of τ vs. V from Fig. 5.

Thus, the question remains: what is the role, if any, of aligned defect-dipoles? As first discussed by Pike et al. [5], we propose that enhanced voltage shifts are an indirect, rather than a direct, result of defect-dipole alignment. As a working model it is proposed that the density of trapped electrons (occupied traps) strongly depends on the value of the polarization. Support for this is that earlier we saw that an enhanced polarization state can lead directly to enhanced electron trapping (Fig. 2). Aligned defect-dipoles will enhance the net polarization, thus *possibly* leading to larger voltage shifts. We strongly state that aligned defect-dipoles may *possibly* lead to large voltage shifts since a larger polarization does not inherently create more defect sites, it simply modulates defect ensemble occupancy by affecting the potential well for the trapped electrons. It is ultimately the number of trapped electrons that determines the extent of the voltage shift.

We briefly discuss some the support for this scenario. (1) The polish-back results of Dimos et al. [4] show that the electron trapping (voltage shift) is near-interfacial, not a bulk phenomenon. (2) The role of aligned defect-dipole complexes in the PZT capacitors can cause the *thermally*-induced voltage shifts to be generally larger than the *optically*-induced shifts in the samples [5,6]. A key difference between these two effects is that vacancy motion can lead to significant alignment of defect-dipoles in long-time or thermally-

accelerated aging studies [4,10,11,14]. Subjecting the capacitor to elevated temperatures with an applied dc bias will enhance the net polarization ($P_D + P_r$) by reorienting defect-dipoles, thereby potentially resulting in greater electron trapping. It may also arise in part since P_r, is also reduced at elevated temperatures. Defect-dipole alignment will not occur during the optical measurements since it is unlikely that appreciable alignment will occur at room temperature during the optical exposure (< 1 min.). (3) Samples prepared with a larger density of defect-dipoles exhibit the largest *thermally*-induced voltage shifts; such samples include those subjected to a reducing ambient [5]. (4) *B*-site donor doping reduces thermally-induced voltage shifts [6,36]. The addition of donor dopant species at the Ti site can reduce the concentration of $V_o^{\bullet\bullet}$ [37,38]. Assuming that the thermally-induced shifts are greater due to the contribution of defect-dipoles involving $V_o^{\bullet\bullet}$, it is expected that processes that reduce the $V_o^{\bullet\bullet}$ density will diminish the voltage shifts enhanced by aligned defect-dipoles. Note, however, that the dopant additions do not reduce the optically-induced voltage shifts as anticipated.

Thus, it appears that the most stringent imprint test involves heating a sample under a dc bias, rather than poling a sample and heating under remanence. This is a more severe imprint test since the applied bias fully polarizes the sample including the defect-dipoles along the electric field direction [5,6,20,30]. These additive processes will enhance the net polarization and potentially lead to the largest voltage shifts.

Defect-dipoles and UV sensitivity

Figure 7 shows the uv sensitivity of the defect-dipoles as a function of illumination time before (a) and after (b) dipole alignment. The defect-dipoles were aligned by a -450V/110°C treatment. The uv light appears to induce charge transfer between the Fe^{1+}-$V_o^{\bullet\bullet}$ dipole complex and the Fe^{3+}-$V_o^{\bullet\bullet}$ complex and thus improving the photosensitivity of this perovskite materials. This may occur since dipole alignment results in an internal field to assist separation of the electronic carrier from the center with which it was activated. This observation will be of interest to those using ferroelectric materials as a photorefractive medium for holographic applications.

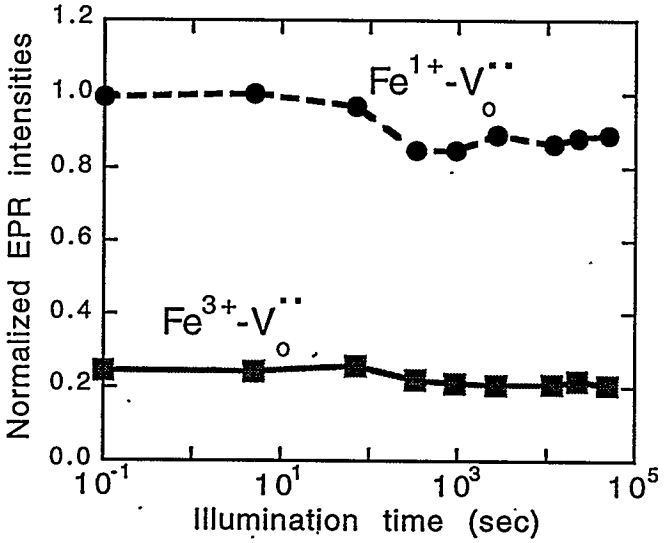

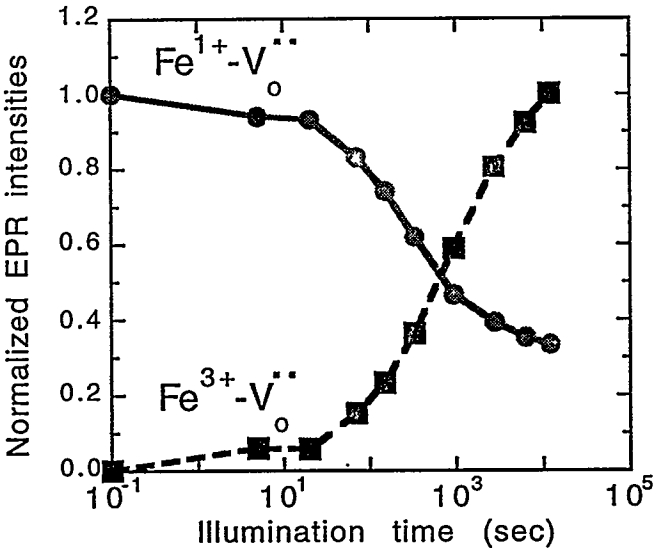

Figure 7: Normalized EPR densities for defect-dipoles before (a) and after (b) alignment as a function of illumination time.

CONCLUSIONS

In summary, we have discussed the processes and mechanisms by which voltage offsets occur in the hysteresis loop of ferroelectric materials. Voltage shifts, which lead to the phenomenon of imprint, are a result of near-interfacial electron trapping. Oxygen vacancies can play an important role, primarily as the mobile component of defect dipoles. However, the alignment of defect-dipoles in and of themselves do not lead to a voltage offset; rather, it leads to a polarization offset that can amplify ferroelectric aging (imprint). It is proposed that the spatial location and occupancy fraction for trapped electrons is determined by the net polarization; however, it is the number of electron trapping sites that ultimately determines the magnitude of the voltage shift.

ACKNOWLEDGMENTS

The portion of this work performed at Sandia National Laboratories was supported by the US Department of Energy under contract DE-AC04-94AL85000 and by DARPA (NCAICM). The UM work is supported by DARPA through Bellcore.

REFERENCES

1. H.D. Megaw, Acta. Cryst. **5**, 739 (1952).
2. J.F. Scott and C.A. Araujo, Science **246**, 1400 (1989).
3. J.T. Evans and R. Womack, IEEE J. Solid State Circuits **23**, 1171 (1988).
4. D. Dimos, W.L. Warren, M.B. Sinclair, B.A. Tuttle, and R.W. Schwartz, J. Appl. Phys. **76**, 4305 (1994).
5. G.E. Pike, W.L. Warren, D. Dimos, B.A. Tuttle, R. Ramesh, J. Lee, V.G. Keramidas, and J.T. Evans, Appl. Phys. Lett. **66**, 484 (1995).
6. W.L. Warren, D. Dimos, G.E. Pike, B.A. Tuttle, M.V. Raymond, R. Ramesh, and J.T. Evans, Jr. Appl. Phys. Lett. **67**, 866 (1995).
7. T. Mihara, H. Watanabe, and C.A. Paz de Arajuo, Jpn. J. Appl. Phys. 32, 4168 (1993).
8. J. Lee, R. Ramesh, V.G. Keramidas, W.L. Warren, G.E. Pike, and J.T. Evans, Jr. Appl. Phys. Lett. **66**, 1337 (1995).

9. P.V. Lambeck and G.H. Jonker, J. Phys. Chem. Solids **47**, 453 (1986).
10. W.A. Schulze and K. Ogino, Ferroelectrics **87**, 361 (1988).
11. G. Arlt and H. Neumann, Ferroelectrics **87**, 109 (1988).
12. R. Lohkamper, H. Neumann, and G. Arlt, J. Appl. Phys. **68**, 4220 (1990).
13. R.D. Pugh, M. J. Sabochick and T.E. Luke, J. Appl. Phys. **72**, 1049 (1992).
14. I.K. Yoo, S.B. Desu, and J. Xing, MRS Symp. Proc. **310**, 165 (1993).
15. H.-J. Hagemann, J. Phys. C **11**, 3333 (1978).
16. P.V. Lambeck and G.H. Jonker, J. Phys. Chem. Sol. 47, 453 (1986).
17. T. Fukami and S. Fujii, Jpn. J. Appl. Phys. **24**, 632 (1985).
18. S.L. Miller, J.R. Schwank, R.D. Nasby, and M.S. Rodgers, J. Appl. Phys. **70**, 2849 (1991).
19. R.A. Assink and R.W. Schwartz, Chem. Mater. **5**, 511 (1993).
20. W.L. Warren, D. Dimos, G.E. Pike, K. Vanheusden, and R. Ramesh, Appl. Phys. Lett. **67**, 1689 (1995).
21. U. Robels, L. Schneider-Stormann, and G. Arlt, Ferroelectrics **168**, 301 (1995).
22. D.M. Smyth, Ferroelectrics, **116**, 117 (1991).
23. N.G. Eror and U. Balachandran, Solid State Commun. **44**, 1117 (1982).
24. E. Siegel and K.A. Müller, Phys. Rev. **B20**, 3587 (1979).
25. E. Siegel and K. A. Müller, Phys. Rev. **B19**, 109 (1979).
26. E. Possenride, P. Jacobs, and O.F. Schirmer, J. Phys. Conden. Matter **4**, 4719 (1992).
27. R.L. Berney and D.L. Cowan, Phys. Rev. **B23**, 37 (1983).
28. W.L. Warren, G.E. Pike, K. Vanheusden, D. Dimos, B.A. Tuttle, and J. Robertson, J. Appl. Phys. **79** xxxx (1996).
29. D. Dimos and W.L. Warren, J. Appl. Phys., submitted.
30. W.L. Warren, K. Vanheusden, D. Dimos, G.E. Pike and B.A. Tuttle, J. Am. Ceram. Soc. **78** (1996).
31. G.V. Lewis, C.R.A. Catlow, and R.E.W. Casselton, J. Am. Ceram. Soc. **68**, 555 (1985).
32. R. M. Waser, J. Am. Ceram. Soc. **72**, 2234 (1989).
33. C. Schaffrin, Phys. Stat. Sol. **A35**, 79 (1976).
34. R. Waser, T. Baiatu, and K.-H. Hardtl, J. Am. Ceram. Soc. **73**, 1645 (1990).
35. W.J. Minford, IEEE TCHMT, **CHMT-5**, 297 (1982).
36. S. Takahashi, Ferroelectrics **41**, 143 (1982).
37. D.M. Smyth, Prog. Solid St. Chem. **15**, 145 (1984).
38. M.V. Raymond, J. Chen, and D.M. Smyth, Integ. Ferroelectrics **5**, 73 (1994)